Review

A review of solar photovoltaic-thermoelectric hybrid system for electricity generation

Guiqiang Li[a, *]

Guiqiang.Li@hull.ac.uk

Samson Shittu[a]

Thierno M.O. Diallo[a]

Min Yu[a]

Xudong Zhao[a, **]

Xudong.zhao@hull.ac.uk

Jie Ji[b]

[a]School of Engineering, University of Hull, Hull HU6 7RX, UK

[b]Department of Thermal Science and Energy Engineering, University of Science and Technology of China, 96 Jinzhai Road, Hefei City, 230026, China

*Corresponding author.

**Corresponding author.

Abstract

Solar energy application in a wider spectrum has the potential for high efficiency energy conversion. However, solar cells can only absorb photon energy of the solar spectrum near the solar cell band-gap energy, and the remaining energy will be converted into thermal energy. The thermoelectric generator is a good choice to utilize this thermal energy. This paper analyses the feasibility of photovoltaic-thermoelectric (PV-TE), and reviews the current types and performance of PV-TE. Furthermore, it presents the optimization and development of PV-TE. In addition, this paper presents the challenge and efficient improvement of PV-TE in actual application. Therefore, this paper would provide a valuable reference for further research into the field of PV-TE and its applications.

Keywords: PV-TE; Wide solar spectrum; Electricity generation; Hybrid solar system

1 Introduction

With the growing concerns about environmental pollution, climate change, and the global fossil energy crisis, research and development of renewable clean energies has received more attention. The sun as one of the renewable energy sources is the most potent source for human kind. This is because the solar radiation that reaches the Earth surface is about 1.2×10^5 TW, which is far greater than the energy consumed by humans [1,2].

The most common way to utilize solar energy is to convert it into two easily harnessed forms; electricity and thermal energy. Apart from photovoltaic (PV) which can convert solar radiations to electricity directly, thermal energy also can be converted to electricity, and one promising method is utilizing the thermoelectric generator (TEG). Thermoelectric (TE) devices have many advantages such as gas-free emissions, solid-state operation, maintenance-free operation without any moving parts and chemical reactions, vast scalability, a long life span of reliable operation and no damage to the environment. Therefore, the combination of PV and TE could be considered to produce more electricity.

Combining a photovoltaic module and a solar thermoelectric generator would enable photons outside the range of a particular solar cell's narrow absorption wavelength to be directed to the TE modules which generates electricity by the thermoelectric effect. Doing this would allow energy conversion efficiency to be increased while simultaneously reducing the heat dissipated by the PV module.

This paper presents a detailed review of the current state of art in solar photovoltaic-thermoelectric hybrid system for electricity generation. It begins with the analysis of the groundwork and feasibility of PV-TE system. An overview of the two main types and

characteristics of PV-TE hybrid system for electricity generation is presented in detail. Furthermore, suggestions on how to optimize and develop PV-TE systems are provided. In addition, the current challenge faced in the application of PV-TE system is discussed and solutions are provided. Therefore, this paper will act as a valuable reference material for research and development of solar PV-TE hybrid systems for electricity generation.

2 Groundwork and feasibility

2.1 A broader spectrum design

The incident broadband solar spectrum is between about 280 nm and 4000 nm. Most solar cells are more efficient when the photon energy of the solar spectrum is near the solar cell band-gap energy. Though the PV panel can directly convert solar energy into electricity, the solar cells cannot fully harness the photons of energy smaller or larger than band-gap energy. For example, Silicon thin-film solar cell (STC) because of its material abundance, promising high performance, potential ability to be low cost and its environmental friendly performance has gained rapid development in recent years. However, its conversion efficiency has the theoretical upper limit estimated to be no greater than 30% [3].

As shown in Fig. 1, photons below the band-gap energy are dissipated as waste heat when they pass through the active area. The photons above the band-gap energy can only be partially utilized while the rest of the energy is converted into waste heat. With the temperature of the panel rising, its efficiency drops as shown in Fig. 2. For example, STC can only absorb sunlight with wavelength up to 800 nm, the remaining sunlight greater than 800 nm cannot be absorbed by PV and would be converted into waste heat which increases the temperature of the panel [5]. This not only decreases the efficiency but also reduces the lifespan of the panel.

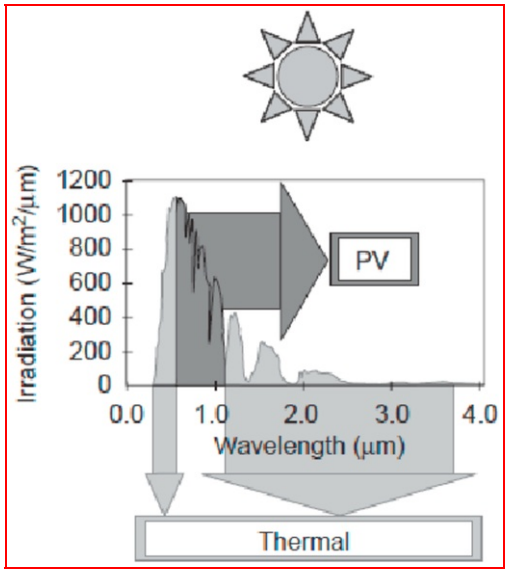

Fig. 1 Splitting the solar spectrum into components for PV and thermal energy conversion [4].

alt-text: Fig. 1

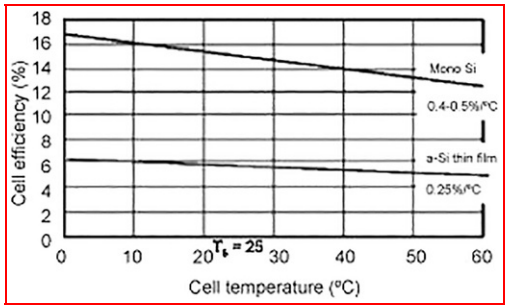

Fig. 2 Relationship between solar cell temperature and efficiency [18].

alt-text: Fig. 2

Thermoelectric generator (TEG) can directly convert thermal energy into electric power, thus the PV-TE hybrid system was proposed. Radiation energy near the band-gap is directly converted to electricity by PV panel and simultaneously, infrared energy is utilized by the TEG to convert heat to electricity. Consequently, more electricity can be produced by the hybrid system than the electricity produced by a single PV or TE system.

The two most common technologies for combining PV and TEG to achieve full solar spectrum utilization are: spectrum splitting photovoltaic-thermoelectric system and integrated photovoltaic-thermoelectric system. Elsarrag et al. developed a spectrum splitting photovoltaic-thermoelectric (PV-TE) system and observed an improved overall performance [6] while Fisac et al. developed an integrated photovoltaic-thermoelectric system to obtain an improved overall efficiency under severe temperature conditions [7].

The combination of PV panel with TEG module can exhaustively absorb a wide range of solar radiation spectrum either in form of infrared energy or ultraviolet energy. Therefore, the concept of photovoltaic–thermoelectric hybrid system is feasible since the method of combining PV with TEG can fully utilize the solar spectrum in theory. This is the greatest advantage of the hybrid system over single PV and TEG system operation respectively.

2.2 PV cell

The PV materials widely used are Silicon, III–V Cells, Thin film chalcogenide, Amorphous/microcrystalline Si, Dye sensitized, Organic, Multi-junction devices. For each PV type, its efficiency is limited. Presently, the common highly efficient photovoltaic cells are the Si (crystalline) of 25.6 ± 0.5% [8], GaAs (thin film) of 28.8 ± 0.9% [9] and Multi-junction devices, InGaP/GaAs/InGaAs of 37.9 ± 1.2% [10] under the global AM1.5 spectrum (1000 W/m^2) at 25 °C. Nevertheless, these PV efficiencies were all affected by the operating temperature significantly.

The temperature increase of solar cells represents a significant issue because of their efficiency decrease [11,12], mostly for solar concentrated systems. An electrical efficiency decrease of about 0.2–0.5% for every 1 °C rise in cell temperature was reported due to the temperature dependence of the open-circuit voltage of the cell depending on the PV material [13–15]. This PV property is known as the temperature coefficient of the PV cell. Table 1 shows the temperature coefficients of various PV technologies along with their typical efficiency [16].

Table 1 Temperature coefficients of different PV cell technologies [16].

alt-text: Table 1

PV technology	T_{ref} (°C)	ηT_{ref} (%)	β_{ref} (C^{-1})	References
Mono-cSi	25	16–24	0.0041	[17]
Poly-cSi	25	14–18	0.004	[18]
a-Si	25	4–10	0.011	[18]
CIS	25	7–12	0.0048	[19]
CdTe	25	10–11	0.00035	[19]

Virtuani et al. measured and compared the relative temperature coefficient of power (γ_{rel}) for different technologies (a-Si based single or multi-junctions, CdTe, CIS, thin-film silicon). They found that, except for the thin film Si device ($\gamma_{rel} = -0.48\%/°C$), compared to the c-Si wafer-based module ($\gamma_{rel} = -0.45\%/°C$) all the studied technologies have lower values of relative temperature coefficient for power. The a-Si single-junction ($\gamma_{rel} = -0.13\%/°C$) device showed the less pronounced decrease with temperature, followed by CdTe ($\gamma_{rel} = -0.21\%/°C$). The microcrystalline and CIGS device gave very close temperature coefficients ($\gamma_{rel} = -0.36\%/°C$) [20]. Fig. 3 shows the impact of temperature on PV maximum power outputs for different PV technologies.

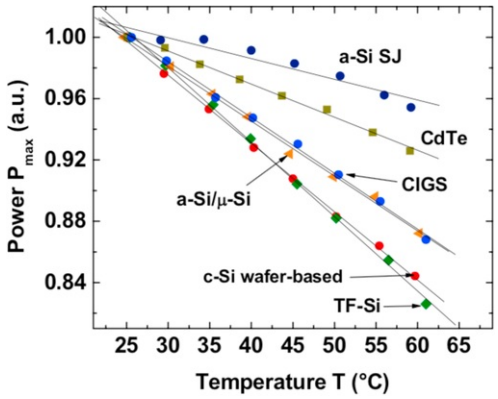

Fig. 3 Impact of temperature on PV maximum power output [20].

alt-text: Fig. 3

Thus, for common solar cells, such as Si based solar cells, their price is cheap but their temperature coefficient is large. Multi-junction solar cells are a possible choice for high temperature operation due to their high efficiency and low temperature coefficient, but their price is high.

2.3 TE material

There are many ways to classify TE materials, one of which is based on temperature. Therefore, TE materials can be divided into three sections. At high temperatures (800–1300 K), ceramics like $BaUO_3$ (ZT = 1.8) [21] and semiconductor SnSe single crystal (ZT = 2.6 ± 0.3) [22] can be used. At middle temperatures (300–800 K), semiconductors like $Bi_2Te_{2.85}Se_{0.15}$ (ZT = 2.38) [23] can be used. At the low temperatures (200–400 K), semiconductors like Bi_2Te_3 (ZT = 2.4) [24] and polymers like 3, 4-ethylenedioxythiophene (ZT = 0.4) [25] at room temperature can be used.

For TE, its theoretical efficiency can be estimated by the following equation:

$$ZT = \frac{\alpha^2}{\kappa}\sigma T \quad (1)$$

where T_C is the cold side temperature, T_H is the hot side and ZT is the Figure of merit.

Applying this equation for low temperatures such as room temperature, for widely used materials which have ZT = 1, the theoretical efficiency for that ZT between the temperature range of 293 K and 373 K is 4%. Considering the highest ZT value of 2.4, the theoretical efficiency for the same condition is 6%. Thus it is of great importance to improve the value of ZT. The dimensionless parameter, ZT, is usually used to determine the performance of a thermoelectric material, as shown in Eq. (2).

$$ZT = \frac{\alpha^2}{\kappa}\sigma T \quad (2)$$

where α is the Seebeck coefficient, σ is electrical conductivity, κ is thermal and T is temperature. As shown in Eq. (2), ZT relates three physical properties intrinsic to the material: the electrical resistivity, σ, the thermopower or Seebeck coefficient, α, and the thermal conductivity, κ. The traditional way to improve ZT is to modify the crystalline structure of the material. It can decrease the thermal conductivity by alloying and/or inserting foreign species to gain good electricity property. Another way is to design novel materials with inherently low thermal conductivity values which would leave the power factor $\frac{\alpha^2}{\sigma}$ the only relevant parameter [26]. It is said that ZT must be greater than 3 to be competitive with traditional generator. The problem is for TE materials, α, σ, κ are dependent. Although theoretically, there is no limitation for developing a TE material with its ZT greater than 3, no such material has ever been found, especially for low temperature. The largest ZT for low temperature ever found is 2.4 at 300 K by growing phonon blocking electron transmitting hetero-structures by low temperature metal organic chemical vapor deposition (MOCVD) technique [27] but the process is complex and the price for that material is high.

For wider application, the method for the development of TE materials must cause the ZT to an attain a high value at a low price. Until now, no such material has ever been found.

3 Types and characteristics of PV-TE hybrid system for electricity generation

3.1 Spectrum splitting PV-TE system

When photon energy is close to the solar cell band-gap energy, spectrum response of several solar cells is usually more efficient. Therefore, photons whose energy is smaller or larger than the solar cell band-gap energy can only be used partly. To solve this problem, spectrum splitting PV-TE systems have been developed because they can enable the utilization of the full solar energy in a very broad solar spectrum wavelength range. With regards to the issue of reducing the PV operating temperature, attention has been drawn to a solar spectrum splitting system in which the PV cells and the thermal processes run in parallel [28]. A spectral beam splitter would only allow the short wavelength solar spectrum to reach the PV receiver, thus substantially reducing both the heat load and the operating temperature of the cell [3].

3.1.1 Spectrum splitting PV-TE system structure

Temperature has a significant opposing effect on the efficiency of the hybrid system given that high temperature difference will lead to a high efficiency for the TEG, however, it would also cause the temperature of the PV to rise and consequently decrease its efficiency. Therefore, the spectrum splitting system was proposed. Generally, the PV-TE splitting system consists of the solar concentrator, the spectrum splitting device, PV module, TE module, and cooling systems as show in Fig. 4.

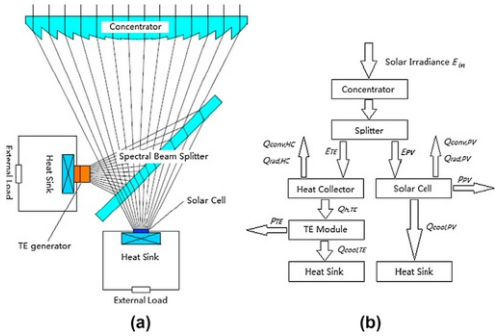

Fig. 4 The PV-TE hybrid system: (a) Schematic diagram of the hybrid system; (b) Energy flow chart of the hybrid system [35].

alt-text: Fig. 4

The spectrum splitting device can divide the sun wavelength into two parts: the suitable wavelength for PV, and the remaining out of range energy for TE. Thus, the temperature of PV can be increased inconspicuously in theory, and the solar concentrator can also be utilized to obtain high heat flux for the TE via Seebeck effect. This would enhance the electricity efficiency of the whole system, and the temperature of the PV plate can be reduced from this procedure.

Li et al. proposed a power system concept for spectrum splitting PV-TE hybrid system. As shown in Fig. 5, the solar spectrum splitter was used to split the incident sunlight for the PV and TE. In order to overcome the discontinuous nature of the solar radiation, a thermal energy storage unit was coupled to system [33].

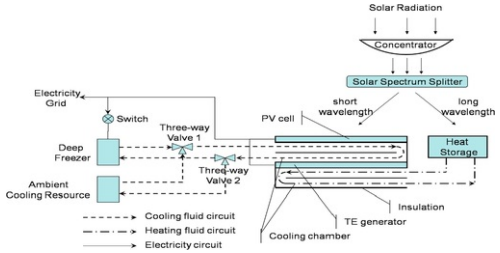

Fig. 5 Schematic of the PV-TE hybrid power system [33].

alt-text: Fig. 5

3.1.2 Spectrum splitting device

The spectrum splitting device is the core of the splitting system. Many types of spectrum splitting techniques have been proposed over the years for solar systems, some of which are: (1) Dichroic splitters (2) Prisms (3) Absorption filters (4) Luminescent concentrators and (5) Holographic concentrators. All these types of splitters mentioned can be used for the spectrum splitting hybrid system with a separate PV receiver and TE generator if different system configurations are employed.

In Fig. 6, the sunlight concentrated by the Fresnel lens was focused on the dichroic beam splitter which split the light into two parts at the cut-off wavelength (λ_s). The wavelength of the photon below λ_s was directed to the concentrated photovoltaic (CPV) cell while the remainder was

directed to the TE. The cut-off wavelength λ_s was determined by the different spectrum splitting devices, which were required to match the PV to reach high efficiency. The converted power fraction of each subsystem when the cut-off wavelength point increases can be seen from the inset [35].

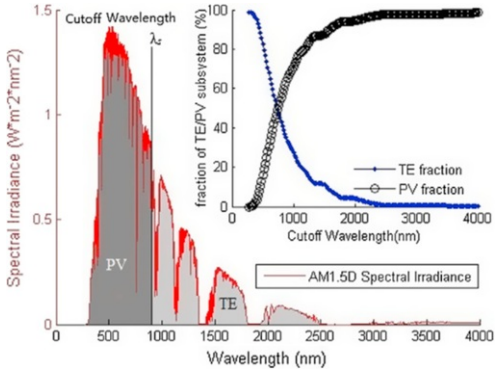

Fig. 6 Segmentation of AM1.5D spectrum in two regions for the CPV subsystem and TEG subsystem [35].

alt-text: Fig. 6

Skjølstrup et al. designed a thin-film multilayer spectral beam splitter for hybrid PV-TE. Thin-film layers of SiO_2 and Si_3N_4 which were deposited on an N BK7 glass were used to construct the beam splitter (shown in Fig. 7). Subsequently, the authors studied the total achievable efficiency versus the number of layers used in the beam splitter while considering from app. 20 to app. 200 layers [32].

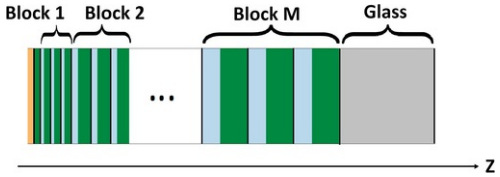

Fig. 7 Schematic of initial design. The first two layers from left represents MgF2 (orange) and SiO2 (dark green), respectively [32].

alt-text: Fig. 7

3.1.3 Splitting PV-TE system performance

For the spectrum splitting photovoltaic-thermoelectric (PV-TE) system, several studies have been carried out. Zhang et al. designed a PV-TE power generating system for a project named “Nano and graded thermoelectric materials/photovoltaic-thermoelectric-wind power generation” [37]. Vorobiev et al. presented the possibility of using spectrum splitting in a PV-TE system and consequently showed this kind of system to be a practical and efficient one [38,39]. In addition, Kraemer et al. presented a general optimization methodology which could be employed in spectrum splitting PV-TE systems. The authors also presented the optimum methodology for cut-off wavelength of such splitting systems and the power fractions of each segment were analysed. Through this study, they found out that the short wavelength region of the solar spectrum which is usually directed to the solar TEG is only a small portion of the total solar spectrum thus, it could be neglected [28]. Furthermore, Fleurial JP stated that highly concentrated PV-TE systems using the spectrum splitting technology can maximize conversion efficiency and improve the overall thermal management [40].

Ju et al. studied the influence of concentration ratio and cooling condition on hybrid PV-TE systems. The authors studied a GaAs $CoSb_3$ hybrid PV-TE system and the relationships between cut-off wavelength, concentration ratio and heat sink performance were discovered. Subsequently, guidelines to follow when designing and optimizing a PV-TE hybrid system were presented. The results showed that the band gaps of the solar cells mainly determined the optimized cut-off wavelength of the whole system. It was discovered that the hybrid system showed a good electrical performance and operated in low temperature range when the solar concentration ratio was ranged between 550 and 770 and the heat transfer coefficient h was between 3000 and 4500 W/m^2K. Furthermore, the TEG subsystem contributed about 10% of the total output power of the GaAs $CoSb_3$ hybrid system therefore, it played a significant role in the power generation. In comparison with the single PV system, the hybrid PV-TE system performed better under high concentration conditions. Considering the cooling condition $h_{cool} = \infty$, maximum solar cell efficiency of the PV-TE hybrid system was around 40% whereas it was only 26% for the single GaAs solar cell [35].

As shown in Fig. 8, the hot side temperature of the TEG sharply decreases with the increase of cut-off wavelength, which decreases the electrical efficiency of the whole system. The hybrid system's efficiency increases with the increase of the concentration ratio and the optimized cut-

off wavelength are almost the same value (Fig. 9). In addition, the maximum overall efficiency increases from 26% to 28%. Compared with the PV-only system, the maximum efficiency of the PV-TE hybrid system increases from 26.62% to 27.49% with the h rising from 3000 to 4500 (Fig. 10). Li et al. used a thermal energy storage unit coupled to the system and their results showed that for high overall efficiency, the system configuration and optimization are the most important factors. Also, their results showed that just by adding a high-grade cold energy storage system under reasonable working conditions, a 30% improvement in the output power could be achieved. The simulation also revealed that a suitable single band-gap PV cell could produce good performance at both peak and off-peak times because it is independent of the operating temperature [33]. The performance of many spectrum splitting PV-TE systems is shown in Table 2.

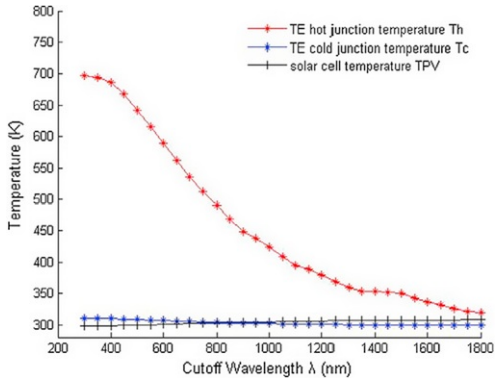

Fig. 8 Working temperature of the hybrid system vs. cut-off wavelength, $C_g = 200$, $h = 10000\ W/m^2K^{-1}$ [35].

alt-text: Fig. 8

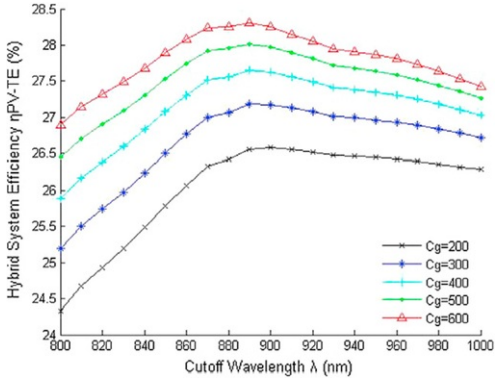

Fig. 9 Hybrid system efficiency vs. cut-off wavelength for different concentration ratio, $h = 10000\ W/m^2K^{-1}$ [35].

alt-text: Fig. 9

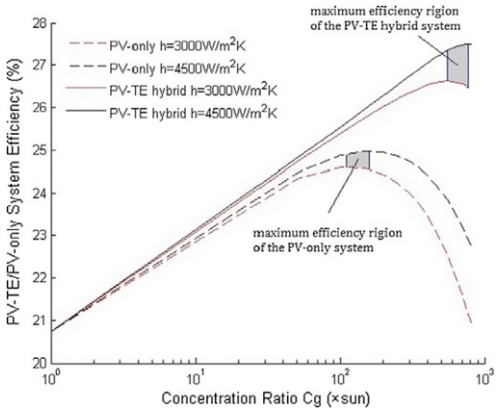

Fig. 10 Comparison of the efficiency between the PV-only system and the PV-TE hybrid system [35].

alt-text: Fig. 10

Table 2 Selected spectrum splitting PV-TE systems.

alt-text: Table 2

Publication year	Affiliation Country	PV type	TE type	PV-TE Efficiency	References
2018	Denmark	c-Si, a-Si, CIGS and CdTe	N/A	~34%	[29]
2017	Italy	a-Si (Amorphous silicon)	N/A	~10%	[30]
2017	Italy	Cu2ZnSnS4 (CZTS)	N/A	~11.25%	[30]
2017	India	N/A	N/A	N/A	[31]
2016	Denmark	Microcrystalline silicon (mc-Si)	N/A	20.20%	[32]
2016	Denmark	a-Si (Amorphous silicon)	N/A	19.40%	[32]
2015	Qatar	Monocrystalline PV cell	Bi2Te3 (HZ-2)	N/A	[6]
2014	UK/China	N/A	N/A	34%	[33]
2012	China/Australia	Si __N (Uxuan Inc.) (c-Si)	N/A	15.30%	[34]
2012	China/Australia	SSRC-C50 (c-Si)	N/A	16.80%	[34]
2012	China/Australia	Heterostructure solar cell	N/A	17.97%	[34]
2012	China/France	GaAs	CoSb3	27.49%	[35]
2012	Japan	a-Si (Amorphous silicon)	Thin film (Bi0.5Sb1.5Te3 and Bi2Te2.7Se0.3)	N/A	[36]

3.2 Integrated PV-TE system

Another type of PV-TE system is the integrated PV-TE system and as shown in Fig. 11, the system consists of a PV module and a TEG module. For some systems a concentrator is usually used to increase the heat flux of the sun irradiation.

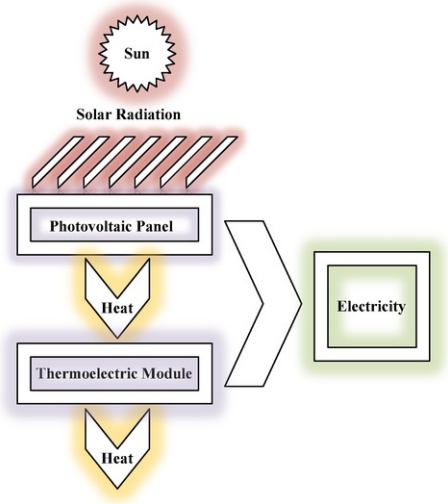

Fig. 11 The Schematic diagram of an integrated system.

alt-text: Fig. 11

3.2.1 Integrated PV-TE system structure

Many research has been done for this type of PV-TE system. These researchers [53–57] attached thermoelectric generators to the back side of PV modules for energy harvesting and the performance of these hybrid systems was investigated theoretically and experimentally in their studies. Van Sark investigated the PV-TE system which attached the TEG to PV modules to convert waste heat into electricity, as shown in Fig. 12. The author also performed a simulation for the simple and idealized model [55].

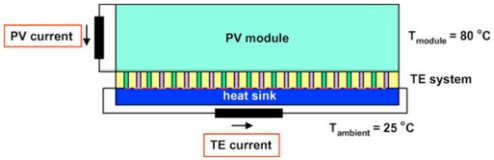

Fig. 12 Schematic overview of the PV-TE hybrid system with multiple thermoelectric generators consisting of n- and p-type doped semiconductor legs [55].

alt-text: Fig. 12

Deng et al. studied an integrated design of a solar-driven hybrid generation system (HGS) and the system consisted of a silicon thin-film solar cell (STC), thermoelectric generators (TEGs) and a heat collector. As seen from Fig. 13, the heat collector collects waste heat from the STC and part of the solar energy, subsequently, this waste heat is transferred to the TEG for thermoelectric conversion. Therefore, it is imperative to include a properly designed heat collector possessing an optimized absorbing layer, conducting layer and insulating layer between the STC and the TEG. The function of the absorbing layer is to collect both solar radiation energy and reflection energy. While the insulating layer prevents heat loss and the conducting layer allows for effective heat conduction [5].

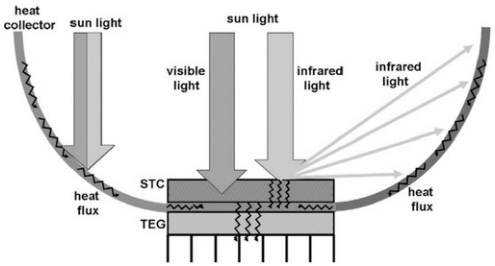

Fig. 13 Schematic diagram of heat flux in HGS [5].

alt-text: Fig. 13

Mohsenzadeh et al. designed a CPV/T + TE hybrid system that included a receiver, parabolic trough reflecting surface and a sun tracking system. The structure of the receiver was such that an equilateral triangle duct was placed in the middle while TE modules and PV arrays were placed at the two lateral sides of the triangular duct and the outer glass cover as shown in Fig. 14 [58].

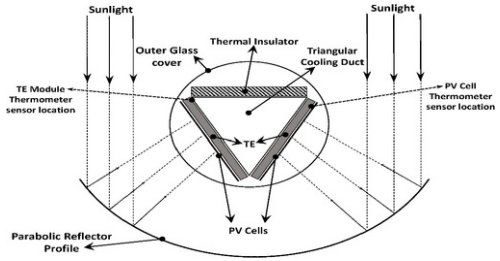

Fig. 14 Schematic diagram of the cross-section of CPV/T + TE hybrid collector [58].

alt-text: Fig. 14

Also, as regards system structure, Soltani et al. presented a tri-generation unit that consisted of a parabolic trough solar collector which was integrated with a solar cell and a thermoelectric generator. The four main parts of the evacuated tube were; glass envelope, photovoltaic tube, thermoelectric tube and absorber pipe (Fig. 15). Furthermore, a TEG module was placed at the back of the PV cell to utilize the waste heat produced from the PV cell. In addition, a single-phase working fluid was flowing inside the absorber tube and this created the temperature gradient across the two ends of the TEG [41].

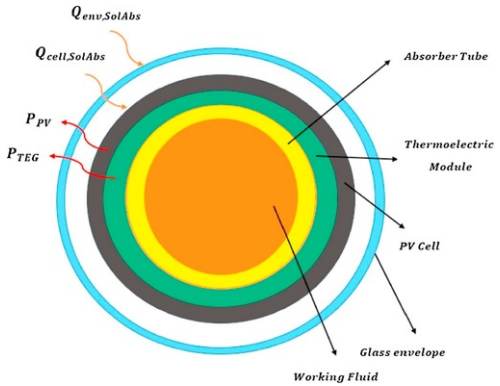

Fig. 15 Cross-sectional view of the evacuated tube [41].

alt-text: Fig. 15

Marandi et al. designed and fabricated a solar cavity packed with hybrid PV-TEG modules (Fig. 16). It was discovered that reduction of the re-radiation loss of the solar radiative power in the cavity receiver led to a temperature increase in the module. Furthermore, the system was tested under solar irradiance that was varied daily for several hours. The authors discovered that the efficiency of the hybrid system reached an all-time high efficiency of around 21.9% at the start of production during the morning hours when the system was exposed to real sunlight [59].

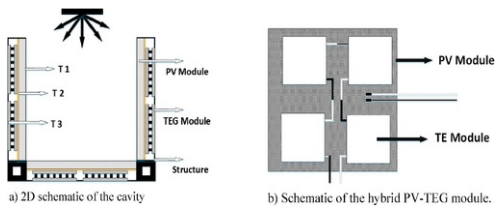

Fig. 16 PV-TEG hybrid system (a) cavity (b) hybrid PV-TEG module [59].

alt-text: Fig. 16

3.2.2 Integrated PV-TE system performance

Deng et al. developed a solar-driven hybrid generation system (HGS) and the results showed that the performance of the TEG and STC are both enhanced for the integrated design. The whole system generated power of 393 mW which was increased by 107.9% compared with that of the single STC [5] and the output power and its increase rate in HGS is shown in Table 3.

Table 3 The output power and its increase rate in HGS [5].

alt-text: Table 3

Module	P_{PV} (mW)	P_{HGS} (mW)	Increase rate (%)	Reference
STC/TEG	189	393	107.9	[5]
PV/TEG	–	–	14.7	[55]
DSC/TEG	9.39	13.8	46.8	[57]
DSC/TEG	39.72	44.26	23	[60]

Furthermore, results obtained by Van Sark showed that the annual performance of the system considered, for the given condition increased by 14.7% and 11%, for Malaga and Utrecht, respectively. In addition, the PV efficiency at 1000 W/m^2 was 10.78% for the given condition. Also, under simulation conditions, the TE efficiency was 3.20%. The research also included the impact of high ZT value on efficiency and it was found that for ZT value of about 3, efficiency could be increased up to 50% [55].

Liao et al. investigated a theoretical model of a hybrid power generation device consisting of a low concentrated photovoltaic (CPV) module and a thermoelectric generator (TEG). The conclusion from this research was that there is an optimum operating condition for some key parameters, such as the thermal conductance between the CPV and the TEG, the current of the CPV, the solar irradiation the concentrating ratio and the figure of merit of the TEG. In addition, the authors found that the efficiency of the system could reach 15% [61].

Xu et al. analysed the performance of a combined system consisting of concentrating photovoltaic/thermal collector and thermoelectric generators. It should be noted that this system had a cooling channel to cool the cold side of the TEG. The results showed that compared with the PV/T system, the PV-TE/T system led to an increase of about 8% efficiency [62]. This result is quite opposite to that of [3]. It suggests that to achieve a better electrical output, cooling of the TEG cold side should be done. The results also showed that the figure of merit has a significant impact on the whole system efficiency. For $Z = 0.00275\ K^{-1}$, PV-TE electrical efficiency of 18.2% was achieved, which was 28% less than that of $Z = 0.00534\ K^{-1}$. This means that exploring new TE materials with high ZT is a promising way to improve the overall performance of the PV-TE hybrid system and decrease the cost per watt. In addition, the results showed that thickness of the TE layer has a positive effect on the whole system. It is true that the thicker the layer is, the less efficient the PV panel is because of the rising temperature of the PV panel. However, the reverse is the case for TEG as the thicker the layer is, the more efficient the TEG becomes. In addition, the result showed that the increase of the TE's efficiency is larger than the amount of the PV's efficiency decrease therefore, the overall efficiency is increased. However, there is a balance between the system temperature and the thickness of the layer because high temperature causes high thermal stress, which decreases the operational life and reliability of system [62].

Naiafi et al. modelled and analysed a combined photovoltaic-thermoelectric power generation system. The results showed that with the increase of the solar radiation, the efficiency of the PV and the efficiency of the TEG show opposite trends for rising temperature values. The performance of the system for a typical summer revealed that the TEG modules generated 28.398 Wh electricity during that day, which was about 1.84% of the total generated electricity by the PV panel during the same time. This means the conversion efficiency of the TEG is rather small. High figure of merit value for TE can significantly improve its conversion efficiency. The results also revealed that the number of the TEG modules has an optimal value [63].

Wu et al. compared the performance of PV-TE with and without glass cover, and the results showed that when $Z = 0.0021\ K^{-1}$, the efficiency of the unglazed PV-TE system was higher than that of the glazed system however, when $Z = 0.0085\ K^{-1}$, the difference in efficiency between both systems decreased gradually as concentration ratio increased [64].

For recent research, the total efficiency of hybrid systems is not largely boosted due to the low conversion efficiency of the TEG. Some of them even show a decrease in the electricity output of the whole system as a result of the poor heat exchange condition of the TEG. Therefore, it is very important to find TE materials with high figure of merit and low cost. Although recent research show that nanomaterials such as super-lattices and nanowires can obtain high ZT, the complex process involved and high price make those material still not widely used. Another thing that can be done to improve the electrical efficiency of the hybrid system is to cool the cold side of the TEG as this can strongly affect the whole system's efficiency. For the structure of the integrated system, it seems that the thickness of the TEG has a positive effect on the conversion efficiency. However, the thermal stress can affect the lifespan of the system. Therefore, it is important to find a balance point taking into consideration all these factors affecting the hybrid system. The performance of many integrated PV-TE systems is shown in Table 4.

Table 4 Selected integrated PV-TE systems.

alt-text: Table 4

Publication year	Affiliation Country	PV type	TE type	PV-TE Efficiency	References
2018	Iran	c-Si	TEC1-12706	~8.25%	[41]
2018	Denmark	c-Si, a-Si, CIGS and CdTe	N/A	~34.2%	[29]
2018	China	N/A	N/A	16.70%	[42]
2018	China/UK	c-Si	N/A	11.04%	[43]
2018	China/UK	GaAs	N/A	22.94%	[43]
2017	China	CIGS	N/A	21.60%	[44]
2017	China	Thin film silicon	N/A	13.10%	[44]
2017	China	a-Si (Amorphous silicon)	N/A	9.10%	[45]
2017	China	Polymer	N/A	8.80%	[45]
2017	Iran/China/UK	c-Si	TEC-1206	~15.5	[46]
2017	China	GaInP2/GaAs/Ge	Bi2Te3	N/A	[47]
2017	Italy	a-Si	N/A	~11%	[30]
2017	Italy	Cu2ZnSnS4 (CZTS)	N/A	~12.25%	[30]
2017	China	GaAs	Bi2Te3 (TEC1-03103)	19.10%	[48]
2016	India	Siemens SP75	N/A	5.80%	[49]
2016	China	GaAs	N/A	18.51%	[50]
2016	Denmark	Silicon (Si) solar cell	Bi2Te3	~16.6%	[51]
2016	India	MAX60 solar cell	Be2Te3	N/A	[52]

4 Optimization and development of PV-TE

The ways to improve the performance of a hybrid PV-TE system are; the use of higher figure of merit (ZT) material for TEG, the use of PV cells with higher efficiency and optimizing thermal management design of the hybrid system [5]. Therefore, PV-TE performance optimization can be classified into two main categories; 1) Material optimization 2) Structural optimization. The performance of hybrid PV-TE system is mainly evaluated in terms of conversion efficiency and electrical power output. The recent optimization and development efforts in the field of PV-TE is shown in Table 5.

Table 5 Selected performance data for some hybrid PV-TE systems.

alt-text: Table 5

PV Properties	TEG Properties			Additional System Components		Operating Conditions			Methodology	System Performance		References	Remarks
Type	Material	Temperature Difference	Figure of Merit (1/K)	Heat Sink/Cooling Medium	Others	Irradiance	Temperature	Conc. Ratio		Overall Efficiency	Overall Power Output		
Multi-junction	N/A	N/A	4	N/A	Concentrator, Solar Tracking System	N/A	300 K	N/A	Theoretical	30%	N/A	[38]	The use of TEG increased efficiency by about 5–10%.
Dye-sensitized solar cell (DSSC)	N/A	N/A	N/A	Air cooled copper based heat sink	Near-infrared (NIR) focusing lens, Hot mirror	100 mW/cm^2	N/A	N/A	Experimental	10% increase	40.02 mW	[60]	Maximum power output and efficiency of the hybrid system were 11.2% and 10% higher than the single DSSC respectively.

Dye-sensitized (DSSC)	N/A	N/A	N/A	N/A	Solar Selective Absorber (SSA)	100 mW/cm^2	N/A	N/A	Experimental	12.80%	12.8 mW/cm^2	[57]	The use of SSA increased the overall efficiency of the hybrid system to 13.8%.
Multi-crystalline silicon	Bi_2Te_3	58 °C	0.004	Air cooled heat sink	N/A	1000 W/m^2	300 K	N/A	Idealized model	23%	~130 W/m^2	[55]	Annual energy increase of about 14.7% and 11% was observed for Malaga and Utrecht respectively.
Dye-sensitized (DSSC)	Bi_2Te_3	N/A	N/A	N/A	N/A	100 mW/cm^2	N/A	N/A	Experimental	28% increase	N/A	[65]	The hybrid system obtained an efficiency increase of 28% compared to conventional TiO2-based DSSC.
Single junction Gallium Arsenide (GaAs)	Skutterudites $CoSb_3$	468.5 K	1.4	Active cooling	Concentrator, Spectral beam splitter		25 °C (ambient)	770 suns	Numerical model	27.49%	0.1905 W	[35]	Performance values of the hybrid system shown were in the optimized range.
Amorphous silicon thin-film	N/A	27 K	N/A	Water cooled aluminium fin heat sink	Heat collector	60 mW/cm^2	310 K (ambient)	N/A	Numerical simulation and Experimental	N/A	393 mW	[5]	The shape of the heat collector (Bowl-shape) ensured a large temperature difference between the TEG sides.
Polymer solar cell (P3HT/IC60B)	Bi_2Te_3	9.5 °C	N/A	Iron heat sink and Ice water	Indium Tin Oxide (ITO) glass	100 mW/cm^2	N/A	N/A	Experimental	N/A	11.29 mW/cm^2	[66]	Output power of hybrid system increased by 46.6% compared to single PV system.
Crystalline Silicon (c-Si)	Bi_2Te_3	15 °C	N/A	Passive heat sink	Thermal conductive paste	100 mW/cm2	25 °C (room temp.)	N/A	Theoretical and Experimental	16.30%	65.2 mW	[67]	Hybrid system efficiency and power output increased by ~ 30% compared to PV cells (12.5%, 50 mW).
Dye-sensitized (DSSC)	N/A	6 K	N/A	N/A	N/A	N/A	N/A	N/A	Equivalent circuit method	24.60%	1.389 mW	[68]	Smaller spacing between thermoelements gives higher output power of TEG.
CuInGaSe2 (CIGS)	Bi2Te3	Cold side temp = 5 °C	N/A	Water	ZnO nanowires	1000 W/m^2	N/A	N/A	Experimental	22% increase	N/A	[69]	For hybrid CIGS PV/TEG, V_{oc} increased from 0.64 V to 0.84 V
Crystalline Silicon (c-Si)	N/A	N/A	N/A	Heat sink with a fan	Optical concentrator	N/A	N/A	16	Theoretical model	~ 18.6%	N/A	[70]	Hybrid system efficiency higher than PV efficiency (18.4%).
Poly crystalline silicon thin film (p-Si TFPV)	N/A	N/A	N/A	Heat sink with a fan	Optical concentrator	N/A	N/A	12	Theoretical model	~ 14%	N/A	[70]	Hybrid system efficiency higher than PV efficiency (11%).
Polymer PV	N/A	N/A	N/A	Heat sink with a fan	Optical concentrator	N/A	N/A	5	Theoretical model	~ 12%	N/A	[70]	Hybrid system efficiency higher than PV efficiency (4%)
Copper indium gallium selenide (CIGS)	N/A	N/A	N/A	Heat sink with a fan	Optical concentrator	N/A	N/A	30	Theoretical model	~ 23.5%	N/A	[70]	Hybrid system efficiency higher than PV efficiency (21.5%).
Single-crystalline silicon	Bi2Te3	N/A	0.003	Air	nano-CUO thin film	1000 W/m^2	300 K (ambient)	N/A	Theoretical model	13%	27% higher than PV	[71]	For figure of merit value above 0.004K^{-1}, the efficiency of the hybrid system can be improved to 30%.
Multijunction (InGaP, InGaAs, Ge)	Bi_2Te_3	4.5 K	1	N/A	Conc. Light	100 mW/cm^2	N/A	20	Experimental and Simulation	32.09%	0.190 W	[72]	Increase in concentration ratio leads to decrease in overall efficiency.
N/A	N/A	Cold side temp = 298 K	N/A	Passive water cooling	Thermal concentrator	1000 W/m^2	298.15 K (ambient)	N/A	Numerical simulation (Matlab)	10.20%	163 mW	[73]	Power output can be increased when PV-TE is operated in vacuum.
N/A	Bi_2Te_3	N/A	0.002	Nanofluid	Glass cover (Glazed)	1000 W/m2	298 K (ambient)	2	Theoretical model	~0.095	~150 W	[64]	Nanofluid increased efficiency by 0.48%.

N/A	Bi_2Te_3	N/A	0.002	Nanofluid	Unglazed	1000 W/m^2	298 K (ambient)	2	Theoretical model	~0.012	~152 W	[64]	Nanofluid increased efficiency by 0.35%.
Perovskite solar cell	Only p-type element	Cold side temp = 300 K	N/A	Air (Convection)	SSA, Conc. light	N/A	300 K (ambient)	N/A	3-D numerical model	18.60%	N/A	[74]	Efficiency of hybrid system (18.6%) was higher than efficiency of single perovskite solar cell (17.8%).
poly-Silicon	Bi_2Te_3	35 °C (Experiment)	N/A	Water	N/A	1000 W/m^2	PV cell temp. varied between 25 °C and 86 °C	N/A	Experimental	N/A	22.50% increase at 86 °C (Theoretical value)	[75]	Shorter thermoelement leg length cools the hybrid system better than longer leg length.
Dye-sensitized	Bi_2Te_3	35 °C (Experiment)	N/A	Water	N/A	1000 W/m^2	86 °C (Maximum operating temp.)	N/A	Experimental and Theoretical	N/A	30.20% increase at 86 °C	[75]	Shorter thermoelement leg length cools the hybrid system better than longer leg length.
Heterojunction solar cell (p type CdTe nanorod, n-type Bi_2Te_3 nanostructure)	n-type Bi_2Te_3 nanostructure	N/A	N/A	N/A	FTO/CdS	100 mW/cm^2	N/A	N/A	Experimental	23.30%	N/A	[76]	The efficiency value obtained (23.30%) was after 1 min illumination.
c-Si	N/A	N/A	0.77	Water cooled heat sink	Optical concentrator (Fresnel), PCM	800 W/m^2 (max)	300 K	100 sun	Theoretical model	20.10%	N/A	[77]	Total efficiency reduced with increase in temperature no matter the value of ZT used (0.77 or 1.5).
CIGS	N/A	N/A	0.77	Water cooled heat sink		800 W/m^2 (max)	300 K	N/A	Theoretical model	20.5	N/A	[77]	No optical concentration was used.
Single-junction GaAs	N/A	N/A	1.5	Water cooled heat sink	Optical concentrator, PCM (Phase change material)	800 W/m^2 (max)	425 K	500 sun	Theoretical model	28.09%	N/A	[77]	Performance of the hybrid system was superior to the single GaAs PV cell and the GaAs PV-TE systems.
GaInP/InGaAs/Ge (III__V)	N/A	N/A	0.77	Water cooled heat sink	Optical concentrator (Fresnel), PCM	800 W/m^2 (max)	300 K	500 sun	Theoretical model	38.90%	N/A	[77]	Addition of PCM helped to maintain system at optimal operating temperature by reducing irradiance fluctuation influence.
Dye-sensitized (DSSC)	p-type $Bi_{0.4}Sb_{1.6}Te_3$ n-type $Bi_2Se_{0.15}Te_3$	N/A	N/A	N/A	N/A	1000 W/m^2	323 K	1 sun	Experimental	9.08%	N/A	[78]	Efficiency of the hybrid system was enhanced by 20.6% and 725.5% in comparison with separate DSSC and TEG respectively
Poly-crystalline	Bi_2Te_3	30	N/A	Heat sink	Micro-channel heat pipe (MCHP)	1000 W/m^2	25 °C (ambient)	N/A	Numerical model	~10.75	N/A	[79]	Efficiency increased by ~30% compared to conventional PV. System efficiency varied with wind velocity and ambient temperature.
Monocrystalline silicon (m-Si)	Bi_2Te_3	5.9 °C	2.4	Water cooled aluminium heat sink	cRIO module	920 W/m^2	31.8 °C (PV)	N/A	Simulation (LabVIEW) and Experimental	18.93%	3.40 mW (TEG)	[80]	m-Si provided the best system performance compared to p-Si and a-Si
Polycrystalline silicon (p-Si)	Bi_2Te_3	5.6 °C	2.4	Water cooled aluminium heat sink	cRIO module	1020 W/m^2	32.9 °C (PV)	N/A	Simulation (LabVIEW) and Experimental	16.71%	3.44 mW (TEG)	[80]	Power gain of 7% when irradiance was increased to 1000 W/m^2
Amorphous silicon (a-Si)	Bi_2Te_3	3.4 °C	2.4	Water cooled aluminium	cRIO module	720 W/m^2	30.8 °C (PV)	N/A	Simulation (LabVIEW)	2.88%	1.12 mW (TEG)	[80]	Power gain of 5% when irradiance was increased to 1000 W/m^2

				heat sink					and Experimental				
Single junction GaAs	Bi_2Te_3	41 °C	N/A	Aluminium heat sink with a fan	Fresnel lens	1000 W/m²	N/A	50 suns	Experimental	~23.2%	N/A	[81]	Hybrid system efficiency increased by ~ 3% compared to single CPV cell (~22.5%)

4.1 Material optimization

The choice of PV and TE materials used can greatly affect the performance of the hybrid system. In the case of PV, the key parameter to be considered is the conversion efficiency of the cell while for TE, figure of merit and temperature range are key parameters to be considered.

The following TE materials can be selected based on the required operating temperature in the hybrid system: a) Bismuth telluride (Bi_2Te_3): $X < 500$ b) Lead telluride (PbTe): $500 \leq X \leq 900$ c) Silicon germanium (Si—Ge): $900 < X \leq 1300$; where X is Temperature in Kelvin [83]. Hybrid system efficiency can be improved by utilizing higher ZT materials. However, the efficiency would remain poor if the thermal loss is still high even if higher ZT materials are used [83]. Improvements in material ZT values by a factor of 2 at least is required to enhance the wide use of TE technology on a large commercial scale [40]. This suggestion is in agreement with [66] and research to develop higher ZT materials is still on-going. Beeri et al. suggested an efficiency enhancement of 50% compared to single PV cell when material with high ZT value of 2.4 is used [72]. Wu et al. argued that not all larger figure of merit values are favourable to a hybrid PV-TE system, depending on some specific system parameters [64]. This finding contradicts the preceding findings discussed therefore, it might be important to carefully choose a material with optimal ZT in order to improve overall system performance.

Different types of PV cells have been used by various researchers in the past with each researcher arguing the comparative advantage of the cell used over others. Perovskite solar cell has been reported by Zhang et al. to achieve a higher efficiency and lower temperature coefficient compared to silicon solar cell and dye-sensitized solar cell (DSSC). The authors estimated the efficiency of a hybrid PV-TE system using perovskite solar cell to be 18.6% while that of a single perovskite solar cell was 17.8% [74]. Kossyvakis et al. found through theoretical investigation that performance enhancement was about 22.5% for the poly-Si and 30.2% for the dye-sensitized based hybrid PV-TE systems respectively at 86 °C [75]. For avoidance of repetition, the different types of PV cells used by various researchers and the corresponding hybrid system performance are shown in Table 5. In particular, silicon and dye-sensitized solar cells have been mostly used in the literature reviewed.

4.2 Structural optimization

The performance of a hybrid PV-TE system can be optimized by changing its structural parameters and the influence of these parameters are discussed in this section. Different methods have been used to optimize the structure of a hybrid PV-TE system and the common ones are; Theoretical model (including numerical simulation) and Experimental model. However, Chen et al. used an uncommon method to optimize the structure of a hybrid PV-TE system. The authors used an Equivalent circuit method and argued that the structure for the best performance of PV and TEG many not be consistent with that for the optimal efficiency of the whole hybrid system [68]. Therefore, it is imperative to determine the structure for the optimal performance of the hybrid system.

Nanostructure has been proposed in recent years and Luo et al. fabricated a solar cell based on heterojunction structure consisting of nanostructured CdTE and Bi_2Te_3. The efficiency of this hybrid system increased by 23% after 1-min illumination [76]. Rai et al. developed an embedded fishnet meta-structure in a hybrid PV-TE system and an efficiency improvement of around 11 folds was observed. The authors also stated that fabricating a 2-D fishnet structure improves efficiency without increasing the size of system [84].

The essential components of a hybrid PV-TE system are; PV cell and TE module. However, more components (e.g. cooling medium, concentrator etc.) can be added to improve the performance of the overall system. The geometric parameters of each of the components in the hybrid system need to be optimized in the interest of obtaining improved overall performance.

4.2.1 PV geometry optimization

Solar energy conversion efficiency can be improved by using nanostructured surfaces because they absorb more irradiance. The cone nanostructures are periodically distributed on the PV surface.

Da et al. used a bio-inspired moth-eye nanostructured surface to reduce the reflection for full solar spectrum photons and an enhanced transmission film was used to improve the transmission for photons with energy below the band-gap energy of the PV cells thereby enabling a substantial utilization of the solar energy spectrum, shown in Fig. 17 [50].

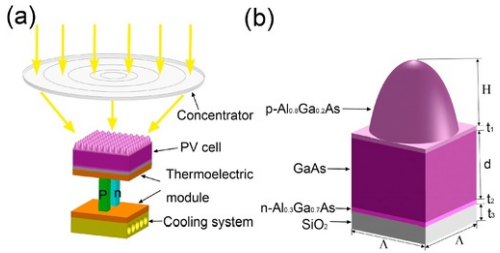

Fig. 17 (a) Schematic diagram of the PV-TE hybrid system with an optical concentrator; (b) the structure of the PV cell within one period [50].

alt-text: Fig. 17

Zhou et al. investigated the effect of the full-spectrum characterisitcs of the nanostructure on the PV-TE hybrid system performances (Fig. 18). Furthermore, moth-eye nanostructures were used on the PV surface to improve the overall conversion efficiency of the PV-TE system (Fig. 19) [85,86].

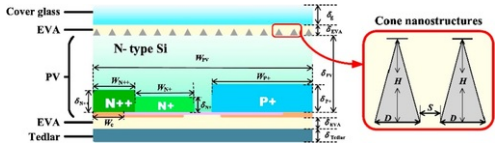

Fig. 18 Detail illustration of the all-back-contact N-type silicon solar cell [85].

alt-text: Fig. 18

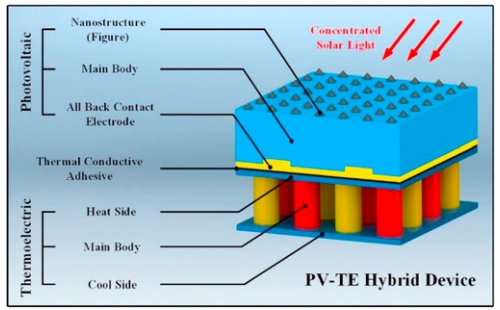

Fig. 19 A tandem PV-TE hybrid device with nanostructured surface [86].

alt-text: Fig. 19

4.2.2 TE geometry optimization

Geometric parameters of the TE (e.g. thermoelement leg length and cross-sectional area) can influence the performance of a hybrid system. The use of thermoelements with shorter length can result in improved power outputs when the hybrid PV-TE system is operated under sufficient illumination [75]. Reducing the side spacing between the thermoelements would result in higher power output from the hybrid system [68]. Surface area reduction in TE modules can increase thermal contact resistance and consequently increase the temperature difference between the different components in the hybrid system [77]. In addition, Hashim et al. discovered that TE modules with smaller cross-sectional area can generate more electrical power than those with a larger cross-sectional area [73]. The geometric parameters used by the authors are shown in Table 6 and the corresponding performance graph obtained is shown in Fig. 20.

Table 6 Geometric parameters of modules investigated [73].

alt-text: Table 6

Module type	N	A_{TE} [mm^2]

I	62	0.64
II	62	1.44
III	62	1.96
IV	62	2.56
V	100	2.56
VI	150	2.56
VII	200	2.56
VIII	250	2.56

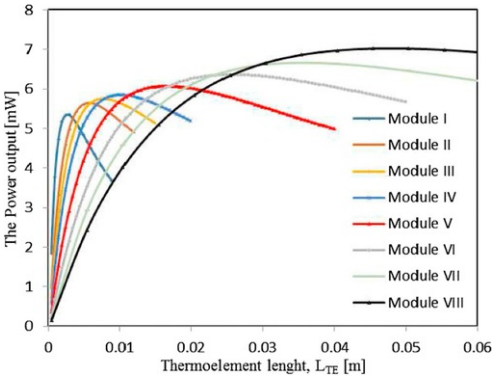

Fig. 20 Power output of different thermoelement length at ambient temperature [73].

alt-text: Fig. 20

Furthermore, Li et al. found that the overall efficiency of the hybrid system decreases as TEG height increases however, the efficiency can increase when the cross sectional area increases to the same TEG height [87]. Therefore, a relationship exists between the performance of a hybrid system and the geometric parameters of the TEG and this is shown in Fig. 21.

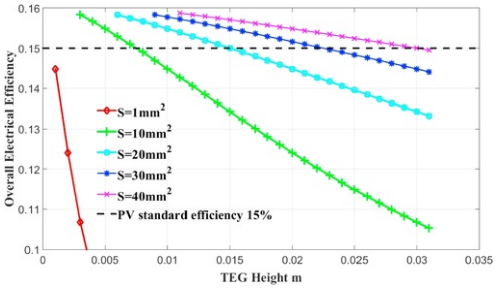

Fig. 21 Hybrid system overall efficiency at different geometric values [87].

alt-text: Fig. 21

To elucidate the significance of finding an optimal geometry for the hybrid system, Li et al. argued that the maximum power output and efficiency of a hybrid PV-TE system occurs when the thermoelements (n and p type) footprint (area) is symmetric however, this is not true for a stand-alone TEG [88]. In the case of a TEG only system, optimal efficiency is achieved when the leg geometry is a trapezoidal shape i.e. Area ratio is not symmetrical [89]. Therefore, it is important for researchers to remember that the optimal design for a TEG only system might not be the same for a hybrid PV-TE system. Finally, future developments in the area of optimizing the thermoelement thickness and module substrate can lead to increase in hybrid system power generation and conversion efficiency [36].

4.2.3 Concentration ratio

Thermal concentration can influence the performance and the cost of hybrid PV-TE systems. Zhang et al. stated that altering thermal concentration can reduce the volume of TEG materials used and consequently reduce the cost of the hybrid system. In addition, the authors found that variation in thermal concentration does not lead to a significant change in the perovskite solar cell thus; the influence of thermal concentration on the efficiency of the hybrid system can be neglected [74]. Cheknane et al. found that the efficiency of InGaP based solar cells used in concentration systems reduces quickly with higher temperature, while working at low insolation levels [90]. Beeri et al. experimentally demonstrated that for concentration factor $X \leq 200$, maximum system efficiency of ~32% can be obtained for the hybrid PV-TE system with the multi-junction PV cell contributing about ~40% of this efficiency at $X \approx 200$ [72]. Fig. 22 provides a graphical illustration of the influence of concentration factor on the performance of the system.

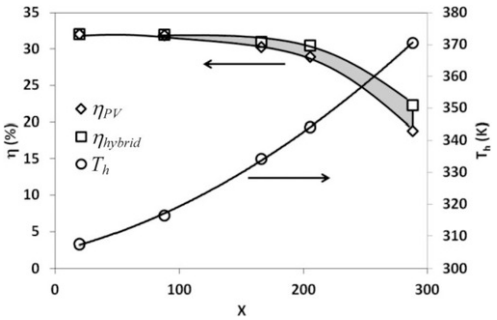

Fig. 22 Electrical efficiency (PV and Hybrid) variation with concentration factor (X) and TEG hot side temperature (T_h) [72].

alt-text: Fig. 22

Incident solar radiation can be adjusted by varying the concentration ratio [28]. Consequently, concentration ratio affects the performance of a hybrid PV-TE system. Zhang et al. found that the efficiency of hybrid system employing different types of solar cells vary with concentration ratio. For example, systems using silicon PV and CIGS PV had an increase in total efficiency when their concentration ratio were increased respectively. However, systems using polymer PV had a reduced total efficiency when concentration ratio was increased [70]. The authors used Fig. 23 to illustrate their findings.

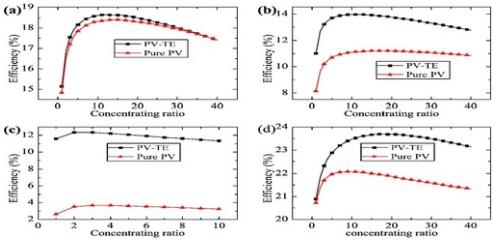

Fig. 23 Efficiency of PV-TE variation with concentration ratio for (a) c-Si PV, (b) p-Si TFPV, (c) polymer PV, (d) CIGS [70].

alt-text: Fig. 23

Ju et al. found that the hybrid PV-TE system is more suitable for working under high concentrations in comparison with a PV only system [35]. This finding is in agreement with [81] as it can be seen clearly from Fig. 24 that the hybrid PV-TE system performs better than the single PV system under high concentrations.

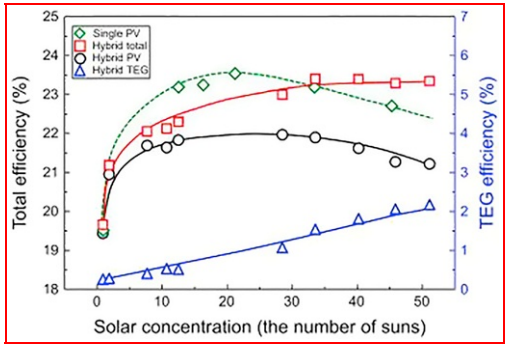

Fig. 24 Comparison of total efficiency with solar concentration [81].

alt-text: Fig. 24

Increasing optical concentration ratio can lead to the improvement of hybrid system performance. This is because an increase in optical concentration ratio causes an increase in maximum power output of the hybrid PV-TE system [61]. In addition, optical concentration as an effect on the hot side temperature and efficiency of a TEG as shown in Fig. 25.

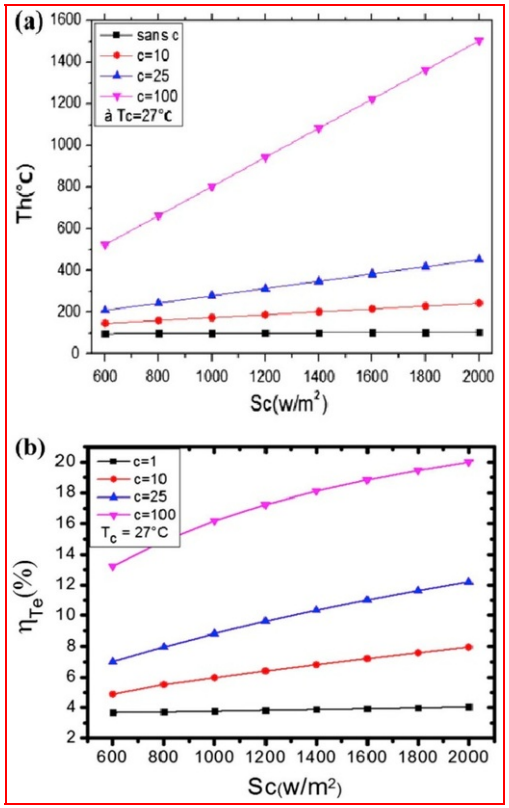

Fig. 25 Optical concentration effect on (a) TEG hot side temperature (b) TEG efficiency [91].

alt-text: Fig. 25

4.2.4 Cooling medium

Cooling of PV cells is a major design requirement as the cells may experience both short term (efficiency loss) and long-term (irreversible damage) degradation due to high temperature [92]. The integration of a cooling medium into hybrid PV-TE system is very important as it can improve the performance of the whole system. Different cooling mediums have been used by researchers in the past and the two most common are; water cooling and air cooling. This can also be seen from Table 5 which shows the cooling medium used in different hybrid system design and the corresponding performance achieved. Kil et al. found that active cooling below ambient temperature is not desirable as it consumes extra energy [81]. Usually, the cooling medium (e.g. water, air) and cooling device (heat sink) are implemented at the bottom of the TEG. Therefore, the cooling methods employed at the cold side of the TEG, affects its heat dissipation capability [5] thus; performance is affected due to the temperature difference created.

Nanofluids have been proposed as an alternative cooling medium. Huminic et al. found through experimental studies that thermal conductivity and viscosity both increase with the addition of nanoparticles [93]. This finding is in agreement with Hajmohammadi et al. who found that the use of Ag and Cu nanoparticles improves cooling performance [94]. Nanofluid improves the system efficiency in comparison with water therefore, it performs better than water [64]. The authors found that nanofluid increased efficiency by 0.35% and 0.48% for the unglazed and glazed systems respectively (Fig. 26).

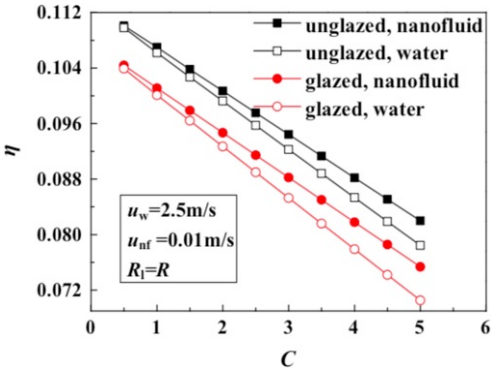

Fig. 26 Variation of system efficiency with concentration adopting different cooling medium [64].

alt-text: Fig. 26

Zhang et al. proposed a new cooling system that can adjust the number of TEG cooled by water in order to decrease the temperature fluctuation caused by the change in solar irradiance. The authors introduced an adjustable cooling block into a hybrid PV-TE system and observed that the power output could be improved [48]. In terms of cooling device, aluminium, copper and iron are some of the materials that have been used in designing a heat sink.

4.3 Others

4.3.1 Load resistance optimization

The influence of load resistance on the performance of a TEG has been examined by various researchers but there is not a substantial amount of research on its influence in the case of hybrid PV-TE systems. A TEG can achieve its maximum power output when its internal resistance is equal to its load resistance [5,87]. Optimizing load resistance of a TEG alone is not suitable for obtaining maximum PV-TE power output. Therefore, the internal resistance of a TE module cannot be used as a reference to match the load resistance for a hybrid PV-TE system [43]. Consequently, it is paramount for researchers to know that the optimal design parameters for a single TEG might not be the same for a hybrid PV-TE system. Lin et al. discovered that smaller TEG load resistance is beneficial to the performance of the hybrid PV-TE system and for optimal performance, TEG load resistance must be greater than TEG internal resistance [71]. This proves the argument that the TEG optimal load resistance is not the same with hybrid PV-TE optimal load resistance.

Kil et al. observed that the efficiency of a CPV cell in a hybrid CPV-TE system varies with load resistance connected to the TEG thus; the efficiency decreases as the load resistance increases [81]. A solution to reduce the influence of load resistance on a hybrid PV-TE system is to implement lossless coupling between the PV and TE devices. Park et al. developed a hybrid PV-TE system with lossless coupling and an overall efficiency improvement of ~30% at 15 °C temperature gradient was achieved [67]. Therefore, load resistance not only affects the power output of a hybrid system but it also affects its efficiency.

Zhang et al. developed the power conditioning circuit using maximum power point tracking so that the output power of the proposed TE–PV hybrid energy system can be maximized, shown in Fig. 27 [95].

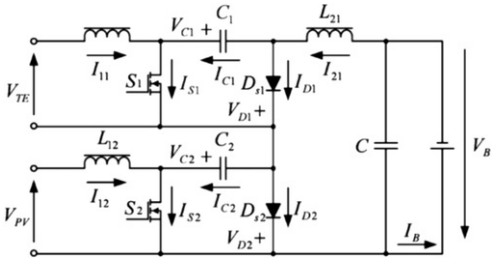

Fig. 27 Proposed Ćuk–Ćuk MIC [95].

alt-text: Fig. 27

4.3.2 New system optimization

Li et al. designed a novel PV-TE system using a flat plate micro-channel heat pipe (MCHP) which could reduce the quantity of TEG used. The PV modules in the system were attached to the upper surface of the MCHP evaporator while the TE modules were attached to the condenser lower surface. During operation, solar energy was imposed on the PV modules located on the MCHP evaporator upper surface, then thermal energy was conveyed to the MCHP condenser by evaporation of the working fluid inside the MCHP. In the condenser, heat was disposed by condensation of the MCHP working fluid and this heat was then transferred to the attached TE modules. This configuration greatly reduced the amount of TEG modules used and also reduced a significant part of the cost thereby showing its comparative advantage over the TE system without heat pipe in series [79].

Cui et al. constructed a novel PV-PCM-TE hybrid system to reduce temperature fluctuations in the PV cells and the TE modules consequently, keep the hybrid system at a fixed operating condition (Fig. 28) [77].

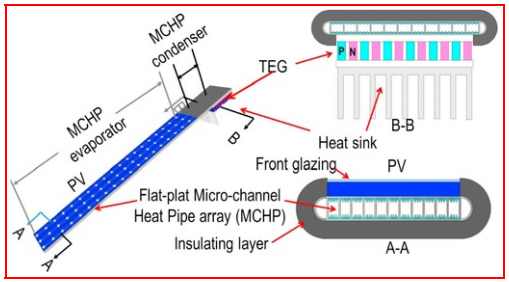

Fig. 28 Schematic diagram of the novel photovoltaic-thermoelectric system [79].

alt-text: Fig. 28

5 Challenge and efficient improvement in actual application

PV and TE materials improvement would play a critical role in the future, however the current challenge is that, efficiency increase by a large margin cannot be accomplished in a short time. Therefore, for actual application, the current realizable efficient improvement based on existing PV and TE modules is significant. There are two methods to overcome this challenge: one is to increase the system efficiency, and the other is to improve the cost performance.

5.1 Enhancing the system efficiency

The key to enhancing the system performance is to couple PV and TE in a way that ensures optimum total conversion efficiency. There has been some different results that indicated that the performance of the coupled system was worse than that of the photovoltaic system alone [39,96]. Bjørk et al. investigated the hybrid system with four different types of PV cells and a universal bismuth telluride TE module theoretically. For c-Si, CIGS and CdTe (Cadmium telluride) PV cells, the hybrid system had a worse performance compared to the pure PV system. In addition, the output power of the coupled system only increased slightly when the a-Si PV cell was used [96].

Therefore, thermal resistance needs to be optimized in actual working conditions (either the thermal resistance between the PV and ambient environment, or the thermal resistance between the PV and TEG, or the thermal resistance between the TEG and ambient environment) so as to overcome the low PV-TE efficiency. Wu et al. analysed a coupled system with and without a glass cover. The authors found that the glazed system could have a better performance than the unglazed coupled system under certain conditions [64].

Zhang et al. studied the impact of thermal contact resistance (TCR) and found that when a small TCR was used, the total efficiency of the hybrid system was higher than that of the PV system alone however, an opposite result was obtained when the TCR was large [70].

Yin et al. studied two main TCRs which were; the TCR between PV cell and TE generator as well as the TCR between TE generator and cooling system. The results obtained showed for different PV cells used, the impacts of the TCR on the hybrid system were similar. In addition, the results showed that a-Si PV cell and polymer PV cell are better for a concentrated hybrid system. Furthermore, it was found that thermal resistance increase can significantly improve the performance of a hybrid system using a-Si PV cell or polymer PV cell [45].

In addition, many researchers have studied the influence of cooling system on hybrid system performance and found that a good cooling system can increase the total coupled system output power and efficiency [46,77].

5.2 Improve the cost performance

It is clear that PV-TE has a higher price than PV alone and it has been mentioned that the TE has a limited contribution to the PV-TE power output since TE has a low electrical efficiency. Therefore, the additional cost of TE still makes the overall system cost high even though the PV price is reducing significantly. Thus, for either the splitting system or integrated system, the system looks economically unfeasible due to the significant higher cost and lower output power of the TE module in comparison to the PV module. However, Li et al. developed a conceptual design of a novel photovoltaic thermoelectric system that saved a lot of TEG modules used by employing the micro-channel heat pipe (Fig. 29). The study indicated that the recovery cost of the extra investment of TE could be achieved in six years which means from the sixth year, the new PV-TE system would be more cost effective compared to the conventional PV system [79].

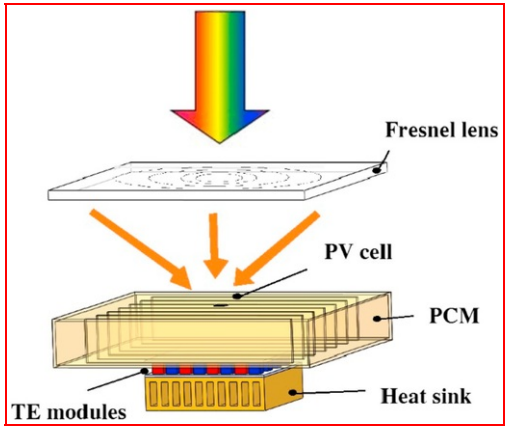

Fig. 29 The proposed PV–PCM–TE hybrid system diagram [77].

alt-text: Fig. 29

6 Conclusion

PV-TE is a solution for solar energy in a wide spectrum, because it can take full advantage of the different power generation principles of PV and TE. The field of PV-TE has received more attention by researchers recently therefore it is experiencing continuous improvements. This review presented the feasibility of PV-TE, common types, material, optimization and development of PV-TEG system, challenge and efficient improvement in actual application. The decrease in cost and increase of conversion efficiency of the PV-TE system positions it to potentially play a great part in contributing to the global efforts for energy conservation and pollutant reduction. In addition, some appropriate future research directions were proposed by the authors. New system designs with high quality processing technology will also enhance the cost effectiveness of PV-TE, which will enable it gain a wide scale application based on the existing materials. In particular, a novel PV-TE system using a flat plate micro-channel heat pipe has shown potential to help reduce the quantity of TEG used significantly and thus, reduce the overall cost of the system. Also, nanofluids as an alternative cooling medium as produced a better performance in comparison with water thus, it could be considered in place of conventional cooling. This review as also shown that the optimal design parameters for a TEG only system might not be the same for a hybrid PV-TE system. Furthermore, nanostructure is gaining more attention and it could significantly improve the efficiency of the PV-TE system. Comprehensive tables showing the most important performance parameters of different PV-TE systems reported in literature have also been presented in this review. In summary, this research has thoroughly reviewed the current state of art in photovoltaic-thermoelectric hybrid system for electricity generation.

Uncited reference

[82].

Acknowledgment

This study was sponsored by the Project of EU Marie Curie International Incoming Fellowships Program (745614), National Key Research and Development Project (2016YFE0124800), Key Projects of International Cooperation of Chinese Academy of Sciences (211134KYSB20160005).

References

[1] G.W. Crabtree and N.S. Lewis, Solar energy conversion, *Phys Today* **60**, 2007, 37–42.

[2] M. Thirugnanasambandam, S. Iniyan and R. Goic, *A review of solar thermal technologies* **vol. 14**, 2010, 312–322.

[3] C.H. Henry, Limiting efficiencies of ideal single and multiple energy gap terrestrial solar cells, *J Appl Phys* **51**, 1980, 4494–4500.

[4] A.G. Imenes and D.R. Mills, Spectral beam splitting technology for increased conversion efficiency in solar concentrating systems: a review, *Sol Energy Mater Sol Cells* **84**, 2004, 19–69.

[5] Y. Deng, W. Zhu, Y. Wang and Y. Shi, Enhanced performance of solar-driven photovoltaic–thermoelectric hybrid system in an integrated design, *Sol Energy* **88**, 2013, 182–191.

[6] E. Elsarrag, H. Pernau, J. Heuer, N. Roshan, Y. Alhorr and K. Bartholome, Spectrum splitting for efficient utilization of solar radiation: a novel photovoltaic–thermoelectric power generation system, *Renew: Wind Water Solar* **2**, 2015, 1–11.

[7] M. Fisac, F.X. Villasevil and A.M. López, High-efficiency photovoltaic technology including thermoelectric generation, *J Power Sources* **252**, 2014, 264–269.

[8] Panasonic Press Release, Panasonic HIT® solar cell achieves world's highest energy conversion efficiency of 25.6% at research level, 2014 http://panasonic.co.jp/corp/news/official.data/data.dir/2014/04/en140410-4/en140410-4.html.

[9] B.M. Kayes, H. Nie, R. Twist, S.G. Spruytte, F. Reinhardt, I.C. Kizilyalli and G.S. Higashi, 27.6% conversion efficiency, a new record for single-junction solar cells under 1 sun illumination, In: *Proceedings of the 37th IEEE photovoltaic specialists conference,* 2011.

[10] K. Sasaki, T. Agui, K. Nakaido, N. Takahashi, R. Onitsuka and T. Takamoto, In: *Proceedings, 9th international conference on concentrating photovoltaics systems, Miyazaki, Japan,* 2013.

[11] J. Wysocki and P. Rappaport, Effect of temperature on photovoltaic solar energy conversion, *J Appl Phys* **31**, 1960, 571–578.

[12] E. Skoplaki and J.A. Palyvos, On the temperature dependence of photovoltaic module electrical performance: a review of efficiency/power correlations, *Sol Energy* **83**, 2009, 614–624.

[13] E. Radziemska, The effect of temperature on the power drop in crystalline silicon solar cells, *Renew Energy* **28**, 2003, 1–12.

[14] D.L. King and P.E. Eckert, Characterizing (rating) the performance of large Photovoltaic arrays for all operating conditions, In: *Proceeding of the 25th IEEE PV specialists conference, Washington, USA,* 1996, 1385–1388.

[15] B. Moshfegh and M. Sandberg, Flow and heat transfer in the air gap behind Photovoltaic panels, *Renew Sustain Energy Rev* **2**, 1998, 287–301.

[16] A. Makki, S. Omer and H. Sabir, Advancements in hybrid photovoltaic systems for enhanced solar cells performance, *Renew Sustain Energy Rev* **41**, 2015, 658–668.

[17] E.C. Kern, Jr. and M.C. Russell, Combined photovoltaic and thermal hybrid collector systems, In: *Proceedings of the 13th IEEEPV specialist conference,* 1978, 1153–1.

[18] X. Zhang, X. Zhao, S. Smitha, J. Xub and X. Yuc, Review of R&D progress and practical application of the solar photovoltaic/thermal(PV/T) technologies, *Renew Sustain Energy Rev* **16**, 2012, 599–61.

[19] J.A. Del Cueto, Comparison of energy production and performance from flat plate Photovoltaic module technologies deployed at fixed tilt, In: *Proceeding of the29th IEEE PV specialists conference, New Orleans, USA,* 2002.

[20] A. Virtuani, D. Pavanello and G. Friesen, Overview of temperature coefficients of different thin film photovoltaic technologies, In: *25th European photovoltaic solar energy conference and exhibition/5th world conference on photovoltaic energy conversion, Valencia, Spain,* 2010.

[21] K. Kurosaki, T. Matsuda, S. Uno, S. Kobayashi and S. Yamanaka, Thermoelectric properties of BaUO3, *J Alloy Comp* **319**, 2001, 271–275.

[22] L.D. Zhao, S. Lo, Y. Zhang, H. Sun, G. Tan, C. Uher, et al., *Ultralow thermal conductivity and high thermoelectric figure of merit in SnSe crystals* **vol. 508**, 2014, 373–377.

[23] T.S. Kim, I.S. Kim, T.K. Kim, S.J. Hong and B.S. Chun, Thermoelectric properties of p-type 25%Bi2Te3 +75%Sb2Te3 alloys manufactured by rapid solidification and hot pressing, *Mater Sci Eng* **90**, 2002, 42–46.

[24] R. Venkatasubramanian, E. Siivola, T. Colpitts and B. O'Quinn, Thin-film thermoelectric devices with high room-temperature figures of merit, *Nature* **413**, 2001, 597–602.

[25] G.H. Kim, L. Shao, K. Zhang and K.P. Pipe, Engineered doping of organic semiconductors for enhanced thermoelectric efficiency, *Nat Mater* 2013, 12.

[26] S. Wang, L. Qing and L. Li, High-temperature thermoelectric properties of Cd1-xPrxO, *Scripta Mater* **69**, 2013, 533–536.

[27] J.H. Seo, D.M. Lee, C.L.K. Park, J.H. Kim and I.A. Nishida, Microstructural and thermoelectric properties of hot-extruded p - t y p e Bi0.5Sb1.5Te3, *Func Grade Mater* 1996, 545–550.

[28] D. Kraemer, L. Hu, A. Muto, X. Chen, G. Chen and M. Chiesa, Photovoltaic-thermoelectric hybrid systems: a general optimization methodology, *Appl Phys Lett* **92**, 2008, 243503.

[29] R. Bjørk and K.K. Nielsen, The maximum theoretical performance of unconcentrated solar photovoltaic and thermoelectric generator systems, *Energy Convers Manag* **156**, 2018, 264–268.

[30] G. Contento, B. Lorenzi, A. Rizzo and D. Narducci, Efficiency enhancement of a-Si and CZTS solar cells using different thermoelectric hybridization strategies, *Energy* **131**, 2017, 230–238.

[31] K.P. Sibin, N. Selvakumar, A. Kumar, A. Dey, N. Sridhara, H.D. Shashikala, et al., Design and development of ITO/Ag/ITO spectral beam splitter coating for photovoltaic-thermoelectric hybrid systems, *Sol Energy* **141**, 2017, 118–126.

[32] E.J.H. Skjølstrup and T. Søndergaard, Design and optimization of spectral beamsplitter for hybrid thermoelectric-photovoltaic concentrated solar energy devices, *Sol Energy* **139**, 2016, 149–156.

[33] Y. Li, S. Witharana, H. Cao, M. Lasfargues, Y. Huang and Y. Ding, Wide spectrum solar energy harvesting through an integrated photovoltaic and thermoelectric system, *Particuology* **15**, 2014, 39–44.

[34] C. Shou, Z. Luo, T. Wang, W. Shen, G. Rosengarten, W. Wei, et al., Investigation of a broadband TiO2/SiO2 optical thin-film filter for hybrid solar power systems, *Appl Energy* **92**, 2012, 298–306.

[35] X. Ju, Z. Wang, G. Flamant, P. Li and W. Zhao, Numerical analysis and optimization of a spectrum splitting concentration photovoltaic–thermoelectric hybrid system, *Sol Energy* **86**, 2012, 1941–1954.

[36] M. Mizoshiri, M. Mikami and K. Ozaki, Thermal–photovoltaic hybrid solar generator using thin-film thermoelectric modules, *Jpn J Appl Phys* **51**, 2012, 06FL07.

[37] Q.J. Zhang, X.F. Tang, P.C. Zhai, M. Niino and C. Endo, Recent development in nano and graded thermoelectric-materials, *Mater Sci Forum* **492–493**, 2005, 135–140.

[38] Y. Vorobiev, J. González-Hernández, P. Vorobiev and L. Bulat, Thermal-photovoltaic solar hybrid system for efficient solar energy conversion, *Sol Energy* **80**, 2006, 170–176.

[39] Y. Vorobiev, J. González-Hernández and A. Kribus, Analysis of potential conversion efficiency of a solar hybrid system with high temperature stage, *J Sol Energy Eng* **128**, 2006, 258–260.

[40] J.P. Fleurial, Thermoelectric power generation materials: technology and application opportunities, *J Miner Metal Mater Soc* **61**, 2009, 79–85.

[41] S. Soltani, A. Kasaeian, T. Sokhansefat and M.B. Shafii, Performance investigation of a hybrid photovoltaic/thermoelectric system integrated with parabolic trough collector, *Energy Convers Manag* **159**, 2018, 371–380.

[42] E. Yin, Q. Li and Y. Xuan, One-day performance evaluation of photovoltaic-thermoelectric hybrid system, *Energy* **143**, 2018, 337–346.

[43] G. Li, K. Zhou, Z. Song, X. Zhao and J. Ji, Inconsistent phenomenon of thermoelectric load resistance for photovoltaic–thermoelectric module, *Energy Convers Manag* **161**, 2018, 155–161.

[44] D. Li, Y. Xuan, Q. Li and H. Hong, Exergy and energy analysis of photovoltaic-thermoelectric hybrid systems, *Energy* **126**, 2017, 343–351.

[45] E. Yin, Q. Li and Y. Xuan, Thermal resistance analysis and optimization of photovoltaic-thermoelectric hybrid system, *Energy Convers Manag* **143**, 2017, 188–202.

[46] S. Soltani, A. Kasaeian, H. Sarrafha and D. Wen, An experimental investigation of a hybrid photovoltaic/thermoelectric system with nanofluid application, *Sol Energy* **155**, 2017, 1033–1043.

[47] K. Teffah and Y. Zhang, Modeling and experimental research of hybrid PV-thermoelectric system for high concentrated solar energy conversion, *Sol Energy* **157**, 2017, 10–19.

[48] J. Zhang and Y. Xuan, Performance improvement of a photovoltaic- Thermoelectric hybrid system subjecting to fluctuant solar radiation, *Renew Energy* **113**, 2017, 1551–1558.

[49] R. Lamba and S.C. Kaushik, Modeling and performance analysis of a concentrated photovoltaic–thermoelectric hybrid power generation system, *Energy Convers Manag* **115**, 2016, 288–298.

[50] Y. Da, Y. Xuan and Q. Li, From light trapping to solar energy utilization: a novel photovoltaic–thermoelectric hybrid system to fully utilize solar spectrum, *Energy* **95**, 2016, 200–210.

[51] A. Rezania, D. Sera and L.A. Rosendahl, Coupled thermal model of photovoltaic-thermoelectric hybrid panel for sample cities in Europe, *Renew Energy* **99**, 2016, 127–135.

[52] V. Verma, A. Kane and B. Singh, Complementary performance enhancement of PV energy system through thermoelectric generation, *Renew Sustain Energy Rev* **58**, 2016, 1017–1026.

[53] H.Y. Yu, Y.Q. Li, Y.H. Shang and B. Su, Design and investigation of photovoltaic and thermoelectric hybrid power source for wireless sensor networks, In: *Proceedings of the 3rd IEEE inter. Conf. On nano/micro engineered and molecular systems, Sanya, China,* 2008, 196–201.

[54] V. Leonov, T. Torfs, R.J.M. Vullers and C.V. Hoof, Hybrid thermoelectric-photovoltaic generators in wireless electroencephalography diadem and electrocardiography shirt, *J Electron Mater* **39**, 2010, 1674–1680.

[55] W.G.J.H.M. Van Sark, Feasibility of photovoltaic–thermoelectric hybrid modules, *Appl Energy* **88**, 2011, 2785–2790.

[56] D. Yang and H. Yin, Energy conversion efficiency of a novel hybrid solar system for photovoltaic, thermoelectric, and heat utilization, *IEEE Trans Energy Convers* **26**, 2011, 662–670.

[57] N. Wang, L. Han, H. He, N.H. Park and K. Koumoto, A novel high-performance photovoltaic-thermoelectric hybrid device, *Energy Environ Sci* **4**, 2011, 3676–3679.

[58] M. Mohsenzadeh, M.B. Shafi and H.F. Mosleh, A novel concentrating photovoltaic/thermal solar system combined with thermoelectric module in an integrated design, *Renew Energy* **113**, 2017, 822–834.

[59] O.F. Marandi, M. Ameri and B. Adelshahian, The experimental investigation of a hybrid photovoltaic-thermoelectric power generator solar cavity-receiver, *Sol Energy* **161**, 2018, 38–46.

[60] X. Guo, Y. Zhang, D. Qin, Y. Luo, D. Li, Y. Pang and Q. Meng, Hybrid tandem solar cell for concurrently converting light and heat energy with utilization of full solar spectrum, *J Power Sources* **195**, 2010, 7684–7690.

[61] T. Liao, B. Lin and Z. Yang, Performance characteristics of a low concentrated photovoltaic- thermoelectric hybrid power generation device, *Int J Therm Sci* **77**, 2014, 158–164.

[62] X. Xu, S. Zhou, M.M. Meyers, B.G. Sammakia and B.T. Murray, Performance analysis of a combination system of concentrating photovoltaic/thermal collector and thermoelectric generators, *J Electron Packag* **136** (4), 2014, 041004.

[63] H. Najafi and K.A. Woodbury, Modeling and analysis of a combined photovoltaic- thermoelectric power generation system, *J Sol Energy Eng* **031013**, 2013, 1–8.

[64] Y.-Y. Wu, S.-Y. Wu and L. Xiao, Performance analysis of photovoltaic-thermoelectric hybrid system with and without glass cover, *Energy Convers Manag* **93**, 2015, 151–159.

[65] T. Chen, G.H. Guai, C. Gong, W. Hu, J. Zhu, H. Yang, Q. Yan and C.M. Li, Thermoelectric Bi2Te3-improved charge collection for high-performance dye-sensitized solar cells, *Energy Environ Sci* **5**, 2012, 6294–6298.

[66] Y. Zhang, J. Fang, C. He, H. Yan, Z. Wei and Y. Li, Integrated energy-harvesting system by combining the advantages of polymer solar cells and thermoelectric devices, *J Phys Chem C* **117**, 2013, 24685–24691.

[67] K.T. Park, S.M. Shin, A.S. Tazebay, H.D. Um, J.Y. Jung, S.W. Jee, et al., Lossless hybridization between photovoltaic and thermoelectric devices, *Sci Rep* **3**, 2013, 1–6.

[68] H. Chen, N. Wang and H. He, Equivalent circuit analysis of photovoltaic – thermoelectric hybrid device with different TE module structure, *Adv Condens Matter Phys* 2014, 1–16.

[69] T. Hsueh, J. Shieh and Y. Yeh, Hybrid Cd-free CIGS solar cell/TEG device with ZnO nanowires, *Prog Photovoltaics Res Appl* **23**, 2015, 507–512.

[70] J. Zhang, Y. Xuan and L. Yang, Performance estimation of photovoltaic-thermoelectric hybrid systems, *Energy* **78**, 2014, 895–903.

[71] J. Lin, T. Liao and B. Lin, Performance analysis and load matching of a photovoltaic-thermoelectric hybrid system, *Energy Convers Manag* **105**, 2015, 891–899.

[72] O. Beeri, O. Rotem, E. Hazan, E.A. Katz and A. Braun, Hybrid photovoltaic-thermoelectric system for concentrated solar energy conversion: experimental realization and modeling, *J Appl Phys* **118**, 2015, 115104.

[73] H. Hashim, J.J. Bomphrey and G. Min, Model for geometry optimisation of thermoelectric devices in a hybrid PV/TE system, *Renew Energy* **87**, 2016, 458–463.

[74] J. Zhang, Y. Xuan and L. Yang, A novel choice for the photovoltaic-thermoelectric hybrid system: the perovskite solar cell, *Int J Energy Res* **40**, 2016, 1400–1409.

[75] D.N. Kossyvakis, G.D. Voutsinas and E.V. Hristoforou, Experimental analysis and performance evaluation of a tandem photovoltaic-thermoelectric hybrid system, *Energy Convers Manag* **117**, 2016, 490–500.

[76] B. Luo, Y. Deng, Y. Wang, M. Gao, W. Zhu, H.T. Hashim, et al., Synergistic photovoltaic-thermoelectric effect in a nanostructured CdTe/Bi2Te3 heterojunction for hybrid energy harvesting, *RSC Adv* **6**, 2016, 114046–114051.

[77] T. Cui, Y. Xuan and Q. Li, Design of a novel concentrating photovoltaic-thermoelectric system incorporated with phase change materials, *Energy Convers Manag* **112**, 2016, 49–60.

[78] Z. Zhou, J. Yang, Q. Jiang, W. Li, Y. Luo, Y. Hou, et al., Large improvement of device performance by a synergistic effect of photovoltaics and thermoelectrics, *Nano Energy* **22**, 2016, 120–128.

[79] G. Li, X. Zhao and J. Ji, Conceptual development of a novel photovoltaic-thermoelectric system and preliminary economic analysis, *Energy Convers Manag* **126**, 2016, 935–943.

[80] D.T. Cotfas, P.A. Cotfas, O.M. Machidon and D. Ciobanu, Investigation of the photovoltaic cell/thermoelectric element hybrid system performance, *IOP Conf Ser Mater Sci Eng* **133**, 2016, 1–10.

[81] T.-H. Kil, S. Kim, D.-H. Jeong, D.-M. Geum, S. Lee, S.-J. Jung, et al., A highly-efficient, concentrating-photovoltaic/thermoelectric hybrid generator, *Nano Energy* **37**, 2017, 242–247.

[82] D.M. Rowe, Thermoelectrics, an environmentally-friendly source of electrical power, *Renew Energy* **16**, 1999, 1251–1256.

[83] W. Zhu, Y. Deng, Y. Wang, S. Shen and R. Gulfam, High-performance photovoltaic-thermoelectric hybrid power generation system with optimized thermal management, *Energy* **100**, 2016, 91–101.

[84] P. Rai, S. Oh, M. Ramasamy and V.K. Varadan, Photonic nanometer scale metamaterials and nanoporous thermoelectric materials for enhancement of hybrid photovoltaic thermoelectric devices, *Microelectron Eng* **148**, 2015, 104–109.

[85] Y.P. Zhou, M.J. Li, W.W. Yang and Y.L. He, The effect of the full-spectrum characteristics of nanostructure on the PV-TE hybrid system performances within multi-physics coupling process, *Appl Energy* **213**, 2018, 169–178.

[86] Y.P. Zhou, Y.L. He, Y. Qiu and Q. Ren, Xie. Multi-scale investigation on the absorbed irradiance distribution of the nanostructured front surface of the concentrated PV-TE device by a MC-FDTD coupled method, *Appl Energy* **207**, 2017, 18–26.

[87] G. Li, X. Chen and Y. Jin, Analysis of the primary constraint conditions of an efficient photovoltaic-thermoelectric hybrid system, *Energies* **10**, 2017, 1–12.

[88] G. Li, X. Chen, Y. Jin and J. Ji, Optimizing on thermoelectric elements footprint of the photovoltaic-thermoelectric for maximum power generation, *Energy Procedia* **142**, 2017, 730–735.

[89] A.S. Al-Merbati, B.S. Yilbas and A.Z. Sahin, Thermodynamics and thermal stress analysis of thermoelectric power generator: influence of pin geometry on device performance, *Appl Therm Eng* **50**, 2013, 683–692.

[90] A. Cheknane, H.S. Hilal, J.P. Charles, B. Benyoucef and G. Campet, Modelling and simulation of InGaP solar cells under solar concentration: series resistance measurement and prediction, *Solid State Sci* **8**, 2006, 556–559.

[91] M. Hajji, H. Labrim, M. Benaissa, A. Laazizi, H. Ez-Zahraouy, E. Ntsoenzok, et al., Photovoltaic and thermoelectric indirect coupling for maximum solar energy exploitation, *Energy Convers Manag* **136**, 2017, 184–191.

[92] A. Royne, C.J. Dey and D.R. Mills, Cooling of photovoltaic cells under concentrated illumination: a critical review, *Sol Energy Mater Sol Cell* **86**, 2005, 451–483.

[93] G. Huminic and A. Huminic, Application of nanofluids in heat exchangers: a review, *Renew Sustain Energy Rev* **16**, 2012, 5625–5638.

[94] M.R. Hajmohammadi, H. Maleki, G. Lorenzini and S.S. Nourazar, Effects of Cu and Ag nano-particles on flow and heat transfer from permeable surfaces, *Adv Powder Technol* **26**, 2015, 193–199.

[95] X. Zhang and K.T. Chau, An automotive thermoelectric–photovoltaic hybrid energy system using maximum power point tracking, *Energy Convers Manag* **52**, 2011, 641–647.

[96] R. Bjørk and K.K. Nielsen, The performance of a combined solar photovoltaic (PV) and thermoelectric generator (TEG) system, *Sol Energy* **120**, 2015, 187–194.

Nomenclature

C_g: Geometrical concentration ratio

h_{cool}: Heat transfer coefficient of cooling system (W/m^2 K)

T: Temperature (T)

T_C: Cold side temperature (K)

T_H: Hot side temperature (K)

Greek symbols

κ : Thermal conductivity (W/m K)

α: Seebeck coefficient (V/K)

σ: Electrical conductivity (S/m)

η: Efficiency (%)

γ_{rel}: Temperature coefficient of power (%/^{o}C)

λ_s: Cut-off wavelength (nm)

Abbreviations

AM: Air Mass

a-Si: Amorphous Silicon

c-Si: Crystalline Silicon

CdTe: Cadmium Telluride

CIGS: Copper Indium Gallium Selenide

CPV: Concentrated Photovoltaic

DSSC: Dye-Sensitized Solar Cell

GaAs: Gallium Arsenide

HGS: Hybrid Generation System

InGaAs: Indium Gallium Arsenide

InGaP: Indium Gallium Phosphide

MCHP: Micro-Channel Heat Pipe

mc-Si: Microcrystalline Silicon

PCM: Phase Change Material

PV: Photovoltaic

PV-TE: Photovoltaic Thermoelectric

SSA: Solar Selective Absorber

STC: Silicon Thin-film Solar Cell

TCR: Thermal Contact Resistance

TE: Thermoelectric

TEG: Thermoelectric Generator

Highlights

- The performance and recent advances in PV-TE are presented.
- The challenge faced in the field of PV-TE and solutions are indicated.
- Current state of art in PV-TE for electricity generation is presented.
- Optimization and development of PV-TE is demonstrated.

Queries and Answers

Query: Please confirm that the provided emails Guiqiang.Li@hull.ac.uk, Xudong.zhao@hull.ac.uk are the correct address for official communication, else provide an alternate e-mail address to replace the existing one, because privat e-mail addresses should not be used in articles as the address for communication.

Answer: Yes.

Query: Please check whether the order of designated corresponding authors are correct, and amend if necessary.
Answer: Yes.

Query: Please check the hierarchy of the headings and sub-headings.
Answer: Yes.

Query: This section comprises references that occur in the reference list but not in the body of the text. Please cite each reference in the text or, alternatively, delete it. Any reference not dealt with will be retained in this section.
Answer: Thank you. In Section 4.1, the first [83] needs to be changed to [82].

Query: Please confirm that given names and surnames have been identified correctly and are presented in the desired order and please carefully verify the spelling of all authors' names.
Answer: Yes

Query: Your article is registered as a regular item and is being processed for inclusion in a regular issue of the journal. If this is NOT correct and your article belongs to a Special Issue/Collection please contact s.venkiteswaran@elsevier.com immediately prior to returning your corrections.
Answer: Yes

Query: The supplied pixels-based source image has a very low image resolution (not enough pixels for the print size) and hence is not directly usable. Please provide us with an image that has a minimum resolution of 300 dots per inch (dpi) and a proper print size. For example, a single column can be around 85 mm wide, and then the raster image needs to be around 900 pixels wide to meet this criterion. It is worthwhile to note that simply upsampling the image to create the right number of pixels will only make the image worse. A better action, most likely, is to export the original image from the software program in which it was put together as an EPS or PDF vector image, or else to export to TIFF by specifying the output print size and resolution in that application, according to these guidelines. You may refer to www.elsevier.com/locate/authorartwork for more details
Answer: Fig. 24 and Fig. 25 have been replaced with higher quality pictures

Query: The supplied pixels-based source image has a very low image resolution (not enough pixels for the print size) and hence is not directly usable. Please provide us with an image that has a minimum resolution of 300 dots per inch (dpi) and a proper print size. For example, a single column can be around 85 mm wide, and then the raster image needs to be around 900 pixels wide to meet this criterion. It is worthwhile to note that simply upsampling the image to create the right number of pixels will only make the image worse. A better action, most likely, is to export the original image from the software program in which it was put together as an EPS or PDF vector image, or else to export to TIFF by specifying the output print size and resolution in that application, according to these guidelines. You may refer to www.elsevier.com/locate/authorartwork for more details
Answer: Fig. 2 has been changed to the best quality picture we can obtain. This picture was obtained from the cited journal paper directly.

Query: The supplied pixels-based source image has a very low image resolution (not enough pixels for the print size) and hence is not directly usable. Please provide us with an image that has a minimum resolution of 300 dots per inch (dpi) and a proper print size. For example, a single column can be around 85 mm wide, and then the raster image needs to be around 900 pixels wide to meet this criterion. It is worthwhile to note that simply upsampling the image to create the right number of pixels will only make the image worse. A better action, most likely, is to export the original image from the software program in which it was put together as an EPS or PDF vector image, or else to export to TIFF by specifying the output print size and resolution in that application, according to these guidelines. You may refer to www.elsevier.com/locate/authorartwork for more details
Answer: Fig. 1 has been changed to the best quality picture we can obtain. This picture was obtained from the cited journal paper directly. By the way, please note that Fig. 28 and Fig. 29 have been interchanged. This is the correct way it should be.